Astrophys Space Sci (2008) 313: 59–63
DOI 10.1007/s10509-007-9589-2

ORIGINAL PAPER

High-resolution mm interferometry and the search for massive protostellar disks: the case of Cep-A HW2

Claudia Comito · Peter Schilke · Ulrike Endesfelder · Izaskun Jiménez-Serra · Jesus Martín-Pintado

Received: 31 January 2007 / Accepted: 9 July 2007 / Published online: 1 September 2007

Abstract The direct detection of accretion onto massive protostars through rotating disks constitutes an important tile in the massive-star-formation-theory mosaic. This task is however observationally very challenging. A very interesting example is Cepheus A HW2. The properties of the molecular emission around this YSO seems to suggest the presence of a massive rotating disk (cf. Patel et al. in Nature 437:109, 2005). We have carried out sub-arcsec-resolution PdBI observations of high-density and shock tracers such as SO_2, SiO, CH_3CN, and CH_3OH towards the center of the outflow. A detailed analysis of the spatial distribution and of the velocity field traced by all observed species leads us to conclude that, on a ∼700 AU scale, the Cep-A "disk" is actually the result of the superposition of multiple hot-core-type objects, at least one of them ejecting an outflow at a small angle with respect to the line of sight. Together with the well-known large-scale outflow ejected by HW2, this setup makes for a very complex spatial and kinematic picture.

Keywords High-mass star formation · Millimeter-wavelength radioastronomy · Millimeter interferometry · High-mass disks

Based on observations carried out with the IRAM Plateau de Bure Interferometer. IRAM is supported by INSU/CNRS (France), MPG (Germany) and IGN (Spain).

C. Comito (✉) · P. Schilke · U. Endesfelder
Max-Planck-Institut für Radioastronomie, Auf dem Hügel 69, 53121 Bonn, Germany
e-mail: ccomito@mpifr-bonn.mpg.de

I. Jiménez-Serra · J. Martín-Pintado
Instituto de Estructura de la Materia, Consejo Superior de Investigaciones Científicas, Departamento de Astrofísica Molecular e Infrarroja, C/Serrano 121, 28006 Madrid, Spain

1 Introduction

Several theories are being considered to explain the formation of massive ($M \geq 8\ M_{\odot}$) stars, which can be roughly grouped into accretion-driven and coalescence-driven models (cf. Stahler et al. 2000). In the latter case, high-mass stars would form by merging of two or more lower-mass objects, making the presence of stable massive accretion disks around the protostar very unlikely. However, only models based on disk-protostar interactions are capable of explaining the existence of jets and outflows: hence, the high incidence, in large samples of massive YSOs, of long, collimated outflows (cf. Beuther et al. 2002) has been interpreted as indirect evidence for the existence of high-mass disks.

It is undoubted that the direct detection of accretion onto massive protostars through rotating disks constitutes an important tile in the massive-star-formation-theory mosaic. From an observational point of view, this task is mainly made difficult by two factors: (i) massive star-forming regions typically are far away, a few kpc on average, making the direct observation of small-scale structure such as disks virtually impossible with current instruments; and (ii), massive stars form in clusters, making the surrounding region extremely complex, both spatially and kinematically.

Although claims of the existence of rotating disks around massive protostars have become popular in the literature, to our knowledge only the case for IRAS 20126+4104 has been convincingly made (cf. Cesaroni et al. 1997, 2005; Zhang et al. 1998; Edris et al. 2005; Sridharan et al. 2005). Cepheus A is also considered a very promising candidate for the detection of a massive disk. Its well-studied bipolar outflow (cf. Gómez et al. 1999, hereafter G99, and references therein) is thought to be powered by the radio-continuum source HW2 ($\sim 10^4\ L_{\odot}$, Rodríguez et al. 1994). The distribution of H_2O masers (Torrelles et al. 1996, hereafter T96) and of the

SiO emission (G99) around HW2, both oriented perpendicularly with respect to the direction of the flow, have been interpreted as strongly supporting the existence of accretion shocks onto a rotating and contracting molecular disk of ∼700 AU diameter, centered on HW2, with the outflow being triggered by the interaction between such disk and HW2 itself. The relative small distance of this region from the Sun (∼725 pc, Johnson 1957) could allow such rotating object to be resolved with interferometric techniques. However, the G99 data did not have enough spatial and spectral resolution to establish a kinematical proof of a disk, and the water masers in T96 share the ambiguity of most similar studies about what the masers actually trace. Based on SMA observations of CH_3CN and dust emission, Patel et al. (2005) have recently claimed the presence of an 8 $M_\odot$ rotating disk, accreting onto HW2, and extending for about 330 AU around the protostar. Our PdBI observations do not support this interpretation: our conclusion is that, on the 1″ scale, the Cep-A "disk" is actually the superposition of at least three different hot-core-type sources, at least one of them being the exciting source for a second molecular outflow.

2 Observations

In 2003 and 2004, with the Plateau de Bure Interferometer in AB (extended) configuration, we have carried out observations of high-density and shock tracers, such as SO_2, SiO, CH_3CN, CH_3OH, $H_2^{18}O$ and HDO towards the HW2 position ($\alpha_{J2000} = 22\ h\ 56\ m\ 17.9\ s$, $\delta_{J2000} = +62°01'49.6''$). High-spectral-resolution correlator units were employed to achieve a channel width of up to ∼0.3 km s^{-1}. A list of some of the observed transitions and beam sizes can be found in Table 1.

3 Results

Figure 1 (upper panel) shows the inner ∼2800 AU of the Cep-A HW2 star-forming region. The peak of the 241 GHz dust emission (grey scale) coincides with the HW2 position and with the center of the large-scale outflow. The integrated CH_3CN emission is also centered on HW2 (contours), and somewhat elongated almost perpendicularly to the direction of the large-scale outflow.

Like other molecular tracers (cf. Comito et al. 2007; Schilke et al. 2007), CH_3CN displays two different velocity components, centered at ∼−5 and ∼−10 km s^{-1} respectively. The solid contours in Fig. 1, lower panel, show the emission of the $CH_3CN(12_3\text{-}11_3)$ transition, integrated between −7 and −3 km s^{-1}, whereas the emission in the range between −11.5 and −7.5 km s^{-1} is represented by the dashed contours (see Sect. 3.2).

Table 1 Summary of observed transitions

Transition	Frequency (GHz)	HPBW
SiO(2-1)	87	2″ × 1.″6
HCN(1-0)	89	1.″9 × 1.″8
$H_2^{18}O(3_{1,3}\text{-}2_{2,0})$	203	1.″0 × 0.″8
SO_2(12-11)	203	1.″0 × 0.″8
^{13}CO(2-1)	220	0.″9 × 0.″7
CH_3CN(12-11)	220	0.″9 × 0.″7
CH_3OH(5-4)	241	0.″7 × 0.″6
$HDO(2_{1,1}\text{-}2_{1,2})$	241	0.″7 × 0.″6

SiO peaks about 0.″3 eastwards of HW2, close to the peak of the −10 km s^{-1} CH_3CN component. A more detailed discussion on this transition can be found in Sect. 3.1.

In what follows, we will discuss in more detail the analysis of the CH_3CN and SiO transitions. Analysis and discussion on the other observed lines will be published in Comito et al. (2007) and Schilke et al. (2007).

3.1 SiO

In spite of the relatively low spatial resolution achieved in the imaging of the 89 GHz SiO line, this transition is the key to understand the dataset. Our data confirm that the spatial distribution of this shock tracer is mainly concentrated in the HW2 region (its presence in the large-scale outflow is limited to a few bullets at large distances from the center), although not centered on the HW2 position. This does indeed suggest that shock processes are taking place in the (projected) immediate vicinities of HW2. However, if the SiO emission were arising from accretion shocks onto a rotating disk (as proposed by G99), we would expect to observe a similar velocity structure to that observed for the other molecular tracers peaking around HW2. Instead, SiO seems to be tracing a completely different kinematic picture: unlike any other line in our dataset, the (2-1) line has a velocity spread of ∼30 km s^{-1} at the zero-flux level (∼15 km s^{-1} FWHM). A mass of about 90 $M_\odot$ would be required to produce such large line width in a gravitationally bound environment (assuming virial equilibrium, and that the emission arises in a region of ∼350 AU radius). This value is about one order of magnitude larger than the estimated mass of HW2, which is expected to be a B0.5 star once in ZAMS (Rodriguez et al. 1994).

We carried out a two-dimensional Gaussian fit of the SiO(2-1) spatial distribution for every spectral channel, thus deriving a distribution of the centroids of SiO emission as a function of velocity. As shown in Fig. 1, lower panel, the centroid positions occupy a well-defined two-lobed area, centered about 0.″3 eastwards of HW2 and of the dust continuum emission peak. Although the error on every single

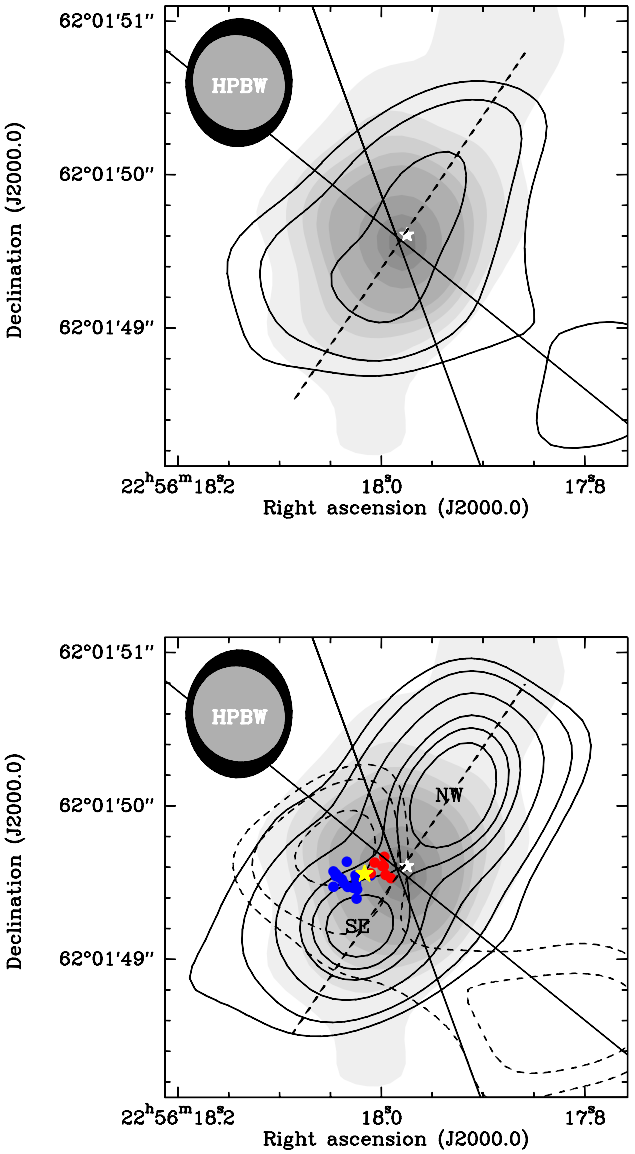

Fig. 1 *Upper and lower panel:* the levels of *grey* represent the dust emission at 241 GHz. Lowest level is 3.3 mJy/beam or 2σ, highest is 22σ. The HW2 position is indicated by the white star. The *solid, crossing lines* show the direction of the large-scale outflow, inferred from our PdBI HCN and ^{13}CO data. The *contours trace* the CH_3CN emission at 220 GHz, and in the top left corner, the HPBW for the dust (*grey foreground*) and CH_3CN (*black background ellipse*) are shown. *Upper panel:* the integrated emission of the $CH_3CN(12_3\text{-}11_3)$ is shown by *solid contours*. *Lower panel:* here the ~ -5 and ~ -10 km s^{-1} velocity components of $CH_3CN(12_3\text{-}11_3)$ are plotted separately (*solid and dashed contours* respectively). The *dots* show the centroid positions for SiO(2-1), *blue-shifted* on the left, *red-shifted* on the right lobe. The yellow star between the SiO lobes points to the position of the Martín-Pintado hot-core

centroid position is large (up to 30%), as a whole their distribution describes a very clear velocity trend, with all the emission at $v_{\rm lsr} < -10$ km s^{-1} clustering in the left lobe, and all the emission at $v_{\rm lsr} > -10$ km s^{-1} clustering in the right lobe. This result suggests that *a second molecular outflow is being ejected in the HW2 region, at a small angle with respect to the line of sight*. Our interpretation is supported by the recent discovery of an intermediate-mass protostar, surrounded by a hot molecular core (Martin-Pintado et al. 2005), at a position which matches perfectly the inferred center position of the SiO outflow (Fig. 1, lower panel), hence a very likely candidate to be its powering engine.

3.2 CH_3CN

The upper panel of Fig. 1 shows the distribution of integrated intensity for the $CH_3CN(12_3\text{-}11_3)$ line. Indeed, the dense molecular gas appears to be distributed around the HW2 position, and elongated in a direction roughly perpendicular to the projected direction of the large-scale outflow on the plane of the sky. From a morphological point of view, therefore, the data are very suggestive of the presence of a $\sim$300 AU-radius disk-like structure around HW2.

The kinematical picture is more complex. A position-velocity cut along the major axis of the elongated structure (indicated in Fig. 1 with a dashed line) reveals a velocity spread of about 6 km s^{-1} (see Fig. 2), also observed by Patel et al. (2005). However, the two intensity peaks along the axis share the same systemic velocity (~ -5 km s^{-1}). The weaker, blue-shifted component of emission (~ -10 km s^{-1}), appears to trace rather the outskirt of a physically separated component than a rotation-induced velocity gradient along the axis of the alleged "disk". The peak of the -10 km s^{-1} CH_3CN emission is spatially and kinematically close to the center of the small-scale SiO outflow (see Fig. 1, lower panel), it may therefore be associated to it and/or to its exciting source.

The CH_3CN integrated intensity is dominated by the two -5 km s^{-1} peaks, which lie respectively about 0.″6 to the northwest, and 0.″5 to the southeast of the HW2 position. In

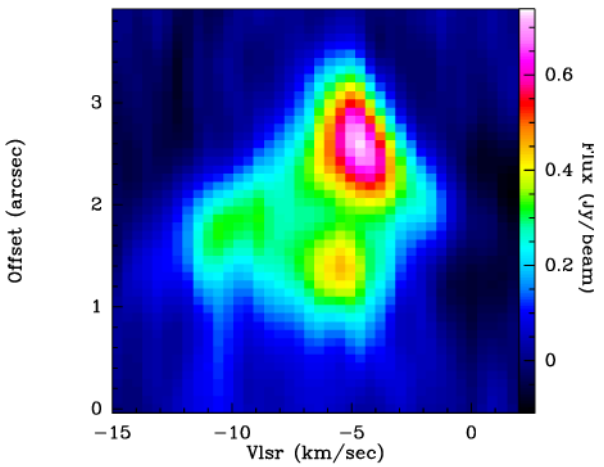

Fig. 2 Position-velocity plot for $CH_3CN(12_3\text{-}11_3)$, along the major axis of the elongated structure (*dashed line* in Fig. 1)

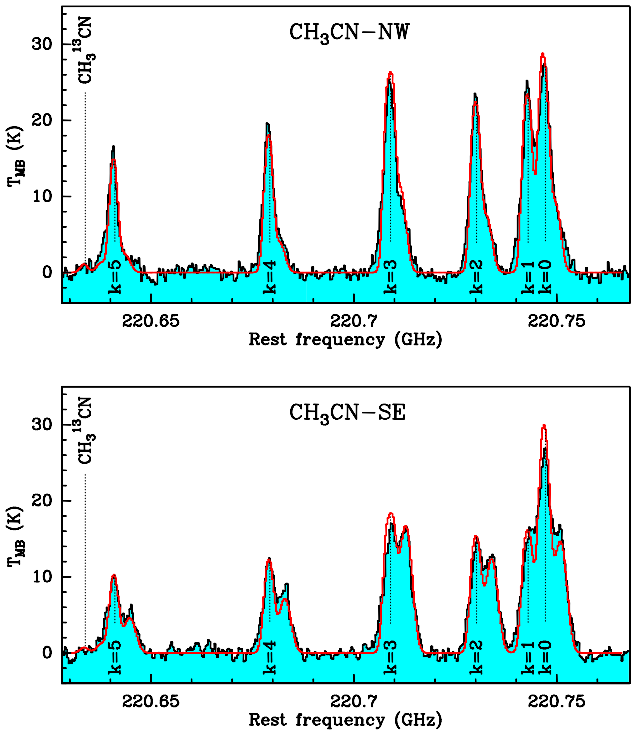

Fig. 3 High-spectral-resolution spectra of the $CH_3CN(12\text{-}11)$ emission at 200 GHz, towards the CH_3CN-NW and -SE positions (see Fig. 1, lower panel). Overlayed in red is the model spectrum, resulting from the parameters listed in Table 2

what follows, we will refer to them respectively as CH_3CN-NW and CH_3CN-SE. Figure 3 compares the spectra observed towards the two positions. It is clear that, in both cases, both the -5 and -10 km s^{-1} components are present along the line of sight, although the contribution from the latter is more intense in the CH_3CN-SE region, i.e., close to the peak of the -10 km s^{-1} SiO emission.

We have assumed LTE approximation to fit the physical parameters associated with the two different velocity components. All transitions in the spectrum are fitted simultaneously, in order to take line blending and optical depth effects properly into account (a detailed description of the method can be found in Comito et al. 2005). At -5 km s^{-1}, the line intensity ratios of the $k = 0$ through $k = 4$ transitions clearly indicate that these lines are optically thick towards both positions. The data at this velocity can only be reproduced by including a very compact, hot, dense object in the model. The emission centered at -10 km s^{-1} can be modeled by a cooler, more extended component. The results of the fit, for the two positions, are summarized in Table 2.

Table 2 LTE model results for the CH_3CN emission towards the NW and SE cores (Fig. 3). For a discussion on the error estimate for these numbers, see Comito et al. (2007)

	v_{lsr} (km s^{-1})	Source size	N(CH_3CN) (cm^{-2})	T_{rot} (K)	Δv (km s^{-1})
CH_3CN-NW	-4.5	0.″3	$\sim 3 \times 10^{16}$	250	2.9
	-8.9	1″	$\sim 8 \times 10^{14}$	150	4.0
CH_3CN-SE	-4.2	0.″25	$\sim 3 \times 10^{16}$	250	3.2
	-10.0	0.″45	$\sim 5 \times 10^{15}$	150	4.5

4 Discussion and open issues

The observed elongation of the molecular gas distribution around HW2, over a radius of $\sim$0.″5 ($\sim$360 AU), appears to be due to the projected superposition, on the plane of the sky, of at least two protostellar objects, of which at least one is triggering a molecular outflow at a small angle with respect to the line of sight (Sects. 3.1, 3.2). All lines in our dataset are consistent with this interpretation (cf. Comito et al. 2007). The observed chemical differentiation between clumps (cf. Brogan et al. 2007; Schilke et al. 2007; Comito et al. 2007) is a further indication of the unlikelihood of a rotating accretion disk over a 1″ spatial extension. A rotating accretion disk around HW2 is likely to exist, but it must be searched for on a smaller scale.

A few questions are still unanswered: first of all, the nature of the CH_3CN-NW and CH_3CN-SE condensations remains to be understood. The analysis of the CH_3CN spectra (Sect. 3.2) seems to suggest the presence of internally heated compact hot-core-type objects. However, the dust emission at 1mm, which peaks unambiguously on the HW2 position and does not show any clumping, does not seem consistent with this picture.

Another open issue is the physical location of the -10 km s^{-1} molecular component. Though it seems likely that the peak of CH_3CN emission is associated with the powering source of the small-scale SiO outflow, its connection to the somewhat more extended molecular emission at this systemic velocity (cf. Brogan et al. 2007) remains to be confirmed.

Although no follow-up studies will be possible from the Atacama site towards the Cep-A East cloud, over a few-hundred AU scale this source provides a very good template for the upcoming ALMA observations of high-mass star-forming regions: in fact, ALMA's high spatial resolution will open a window on a new degree of complexity for massive star-forming regions, in which what currently is known as giant massive hot-core-type sources is likely to break up in a cluster of dozens of smaller sources.

References

Beuther, H., et al.: Astron. Astrophys. **387**, 931 (2002)
Brogan, C., et al.: Astrophys. Space Sci. (2007). doi: 10.1007/s10509-007-9598-1

Cesaroni, R., et al.: Astron. Astrophys. **325**, 525 (1997)
Cesaroni, R., et al.: Astron. Astrophys. **434** (2005)
Comito, C., et al.: Astrophys. J. Suppl. Ser. **156**, 127 (2005)
Comito, C., et al.: Astron. Astrophys. **469**, 207 (2007)
Edris, K.A., et al.: Astron. Astrophys. **434**, 213 (2005)
Gómez, J.F., et al.: Astrophys. J. **514**, 287 (1999)
Johnson, H.L.: Astrophys. J. **126**, 121 (1957)
Martín-Pintado, J., et al.: Astrophys. J. Lett. **628**, L61 (2005)
Patel, N.A., et al.: Nature **437**, 109 (2005)
Rodríguez, L.F., et al.: Astrophys. J. **430**, L65 (1994)
Schilke, P., et al.: In preparation
Sridharan, T.K., Williams, S.J., Fuller, G.A.: Astrophys. J. Lett. **631**, L73 (2005)
Stahler, S.W., et al.: In: Mannings, V., Boss, A.P., Russel, S.S. (eds.) Protostars and Planets IV, p. 327. University of Arizona Press, Tucson (2000)
Torrelles, J.M., et al.: Astrophys. J. **457**, L107 (1996)
Zhang, Q., et al.: Astrophys. J. **505**, L151 (1998)